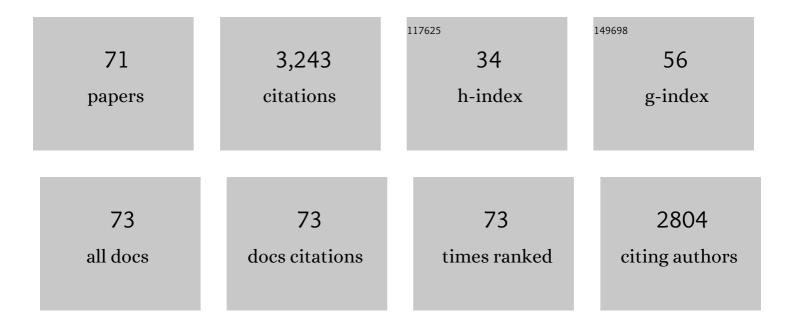
Kathryn J Wahl

List of Publications by Year in descending order

Source: https://exaly.com/author-pdf/1515734/publications.pdf Version: 2024-02-01



ΚΑΤΗΡΥΝΙΙΛΛΑΗ

#	Article	IF	CITATIONS
1	Predicting the corrosion-wear response of an isolated austenite phase under anodic polarization. Wear, 2022, 494-495, 204249.	3.1	1
2	Tribocorrosion Behavior of 2205 Duplex Stainless Steel in Sodium Chloride and Sodium Sulfate Environments. Tribology Letters, 2022, 70, .	2.6	3
3	Comparative analysis of stalked and acorn barnacle adhesive proteomes. Open Biology, 2021, 11, 210142.	3.6	13
4	Distribution of Select Cement Proteins in the Acorn Barnacle Amphibalanus amphitrite. Frontiers in Marine Science, 2020, 7, .	2.5	8
5	Direct Observation of Corrosive Wear by <i>In Situ</i> Scanning Probe Microscopy. ACS Applied Materials & amp; Interfaces, 2020, 12, 23543-23553.	8.0	6
6	Pressure cycling technology for challenging proteomic sample processing: application to barnacle adhesive. Integrative Biology (United Kingdom), 2019, 11, 235-247.	1.3	20
7	Comparison of seven methods for DNA extraction from prosomata of the acorn barnacle, Amphibalanus amphitrite. Analytical Biochemistry, 2019, 586, 113441.	2.4	2
8	Adhesion of acorn barnacles on surface-active borate glasses. Philosophical Transactions of the Royal Society B: Biological Sciences, 2019, 374, 20190203.	4.0	11
9	Insights into tribology from in situ nanoscale experiments. MRS Bulletin, 2019, 44, 478-486.	3.5	34
10	Molecular Recognition of Structures Is Key in the Polymerization of Patterned Barnacle Adhesive Sequences. ACS Nano, 2019, 13, 5172-5183.	14.6	32
11	Below the Hall–Petch Limit in Nanocrystalline Ceramics. ACS Nano, 2018, 12, 3083-3094.	14.6	105
12	Acorn Barnacles Secrete Phaseâ€5eparating Fluid to Clear Surfaces Ahead of Cement Deposition. Advanced Science, 2018, 5, 1700762.	11.2	52
13	Marine Biofouling: Acorn Barnacles Secrete Phase-Separating Fluid to Clear Surfaces Ahead of Cement Deposition (Adv. Sci. 6/2018). Advanced Science, 2018, 5, 1870038.	11.2	0
14	Characterization of longitudinal canal tissue in the acorn barnacle Amphibalanus amphitrite. PLoS ONE, 2018, 13, e0208352.	2.5	12
15	High-performance nanomaterials formed by rigid yet extensible cyclic Î ² -peptide polymers. Nature Communications, 2018, 9, 4090.	12.8	15
16	Mild Solvothermal Growth of Robust Carbon Phosphonitride Films. Chemistry of Materials, 2018, 30, 6082-6090.	6.7	2
17	Barnacle biology before, during and after settlement and metamorphosis: a study of the interface. Journal of Experimental Biology, 2017, 220, 194-207.	1.7	39
18	Oxidase Activity of the Barnacle Adhesive Interface Involves Peroxide-Dependent Catechol Oxidase and Lysyl Oxidase Enzymes. ACS Applied Materials & Interfaces, 2017, 9, 11493-11505.	8.0	61

KATHRYN J WAHL

#	Article	IF	CITATIONS
19	Effect of aging of 2507 super duplex stainless steel on sliding tribocorrosion in chloride solution. Wear, 2017, 380-381, 251-259.	3.1	21
20	Electron Enhanced Growth of Crystalline Gallium Nitride Thin Films at Room Temperature and 100 °C Using Sequential Surface Reactions. Chemistry of Materials, 2016, 28, 5282-5294.	6.7	41
21	Imaging Active Surface Processes in Barnacle Adhesive Interfaces. Langmuir, 2016, 32, 541-550.	3.5	31
22	Sequence basis of Barnacle Cement Nanostructure is Defined by Proteins with Silk Homology. Scientific Reports, 2016, 6, 36219.	3.3	79
23	Coating/substrate interaction in elastomer-steel bilayer armor. Journal of Composite Materials, 2016, 50, 2853-2859.	2.4	8
24	Surfaceâ€Active Borate Classes as Antifouling Materials. Advanced Materials Interfaces, 2015, 2, 1500370.	3.7	2
25	Molt-dependent transcriptomic analysis of cement proteins in the barnacle Amphibalanus amphitrite. BMC Genomics, 2015, 16, 859.	2.8	46
26	Shell Structure and Growth in the Base Plate of the Barnacle <i>Amphibalanus amphitrite</i> . ACS Biomaterials Science and Engineering, 2015, 1, 1085-1095.	5.2	10
27	Self-Assembly of Protein Nanofibrils Orchestrates Calcite Step Movement through Selective Nonchiral Interactions. ACS Nano, 2015, 9, 5782-5791.	14.6	27
28	Electron Backscatter Diffraction (EBSD) Study of the Structure and Crystallography of the Barnacle Balanus amphitrite. Jom, 2014, 66, 143-148.	1.9	11
29	Growth and development of the barnacle <i>Amphibalanus amphitrite</i> : time and spatially resolved structure and chemistry of the base plate. Biofouling, 2014, 30, 799-812.	2.2	55
30	Positively 'negative' friction. Nature Materials, 2012, 11, 1004-1005.	27.5	2
31	Divalent–Anion Salt Effects in Polyelectrolyte Multilayer Depositions. Langmuir, 2012, 28, 15831-15843.	3.5	46
32	Optical Spectroscopy of Marine Bioadhesive Interfaces. Annual Review of Analytical Chemistry, 2012, 5, 229-251.	5.4	17
33	Barnacle Balanus amphitrite Adheres by a Stepwise Cementing Process. Langmuir, 2012, 28, 13364-13372.	3.5	54
34	Fabrication and Response of Laser-Printed Cavity-Sealing Membranes. Journal of Microelectromechanical Systems, 2011, 20, 436-440.	2.5	13
35	Barnacles resist removal by crack trapping. Journal of the Royal Society Interface, 2011, 8, 868-879.	3.4	25

36 Macroscale to Microscale Tribology. , 2011, , 5-22.

KATHRYN J WAHL

#	Article	IF	CITATIONS
37	A Nano- to Macroscale Tribological Study of PFTS and TCP Lubricants for Si MEMS Applications. Tribology Letters, 2010, 38, 69-78.	2.6	16
38	In Situ Studies of TiC1â^'x N x Hard Coating Tribology. Tribology Letters, 2010, 40, 365-373.	2.6	20
39	Measurement of Contractile Stress Generated by Cultured Rat Muscle on Silicon Cantilevers for Toxin Detection and Muscle Performance Enhancement. PLoS ONE, 2010, 5, e11042.	2.5	74
40	Characterization of the Adhesive Plaque of the Barnacle <i>Balanus amphitrite</i> : Amyloid-Like Nanofibrils Are a Major Component. Langmuir, 2010, 26, 6549-6556.	3.5	178
41	Mechanical anisotropy of nanostructured parylene films during sliding contact. Journal Physics D: Applied Physics, 2010, 43, 045403.	2.8	27
42	Computational design of thin-film nanocomposite coatings for optimized stress and velocity accommodation response. Wear, 2009, 267, 1137-1145.	3.1	10
43	Microstructural modeling of adaptive nanocomposite coatings for durability and wear. Wear, 2009, 266, 1003-1012.	3.1	8
44	<i>In situ</i> ATR–FTIR characterization of primary cement interfaces of the barnacle <i>Balanus amphitrite</i> . Biofouling, 2009, 25, 359-366.	2.2	60
45	Role of Surfactant in the Stability of Liquid Crystal-Based Nanocolloids. Langmuir, 2009, 25, 2419-2426.	3.5	18
46	Barnacle cement: a polymerization model based on evolutionary concepts. Journal of Experimental Biology, 2009, 212, 3499-3510.	1.7	131
47	Quantitative in situ measurement of transfer film thickness by a Newton's rings method. Wear, 2008, 264, 731-736.	3.1	52
48	Run-in behavior of nanocrystalline diamond coatings studied by in situ tribometry. Wear, 2008, 265, 477-489.	3.1	71
49	Processing and mechanical performance of liquid crystalline polymer/nanofiber monofilaments. Scripta Materialia, 2008, 58, 25-28.	5.2	7
50	Base plate mechanics of the barnacleBalanus amphitrite(=Amphibalanus amphitrite). Biofouling, 2008, 24, 109-118.	2.2	43
51	Observing Interfacial Sliding Processes in Solid–Solid Contacts. MRS Bulletin, 2008, 33, 1159-1167.	3.5	45
52	Accessing Inaccessible Interfaces: <i>In Situ</i> Approaches to Materials Tribology. MRS Bulletin, 2008, 33, 1145-1150.	3.5	71
53	Nanocrystalline soft magnetic ribbons with high relative strain at fracture. Applied Physics Letters, 2007, 90, 212508.	3.3	20
54	In situ tribometry of solid lubricant nanocomposite coatings. Wear, 2007, 262, 1239-1252.	3.1	66

KATHRYN J WAHL

#	Article	IF	CITATIONS
55	In Situ Analysis of Third Body Contributions to Sliding Friction of a Pb–Mo–S Coating in Dry and Humid Air. Tribology Letters, 2007, 28, 263-274.	2.6	53
56	Preparation of chameleon coatings for space and ambient environments. Thin Solid Films, 2007, 515, 6737-6743.	1.8	73
57	Oscillating adhesive contacts between micron-scale tips and compliant polymers. Journal of Colloid and Interface Science, 2006, 296, 178-188.	9.4	99
58	A comparison of JKR-based methods to analyze quasi-static and dynamic indentation force curves. Journal of Colloid and Interface Science, 2006, 298, 652-662.	9.4	134
59	Anisotropic nanomechanical properties of Nephila clavipes dragline silk. Journal of Materials Research, 2006, 21, 2035-2044.	2.6	21
60	Analysis of rail surfaces from a multishot railgun. IEEE Transactions on Magnetics, 2005, 41, 211-213.	2.1	44
61	Nanomechanical and Microstructural Properties of Bombyx mori Silk Films. Materials Research Society Symposia Proceedings, 2004, 844, 1.	0.1	1
62	Nanomechanical and Microstructural Properties of <i>Bombyx mori</i> Silk Films. Materials Research Society Symposia Proceedings, 2004, 841, R2.2.1/Y2.2.1.	0.1	3
63	Silica aerogels with enhanced durability, 30-nm mean pore-size, and improved immersibility in liquids. Journal of Non-Crystalline Solids, 2004, 350, 244-252.	3.1	44
64	Quantitative imaging of nanoscale mechanical properties using hybrid nanoindentation and force modulation. Journal of Applied Physics, 2001, 90, 1192-1200.	2.5	242
65	Superlow friction behavior of diamond-like carbon coatings: Time and speed effects. Applied Physics Letters, 2001, 78, 2449-2451.	3.3	230
66	Measuring nanomechanical properties of a dynamic contact using an indenter probe and quartz crystal microbalance. Journal of Applied Physics, 2001, 90, 6391-6396.	2.5	69
67	Effects of ion implantation on microstructure, endurance and wear behavior of IBAD MoS2. Wear, 2000, 237, 1-11.	3.1	46
68	Wear behavior of Pb–Mo–S solid lubricating coatings. Wear, 1999, 230, 175-183.	3.1	116
69	Quantification of a lubricant transfer process that enhances the sliding life of a MoS2 coating. Tribology Letters, 1995, 1, 59-66.	2.6	100
70	Low-friction, high-endurance, ion-beam-deposited Pbî—,Moî—,S coatings. Surface and Coatings Technology, 1995, 73, 152-159.	4.8	94
71	Design and calibration of a scanning force microscope for friction, adhesion, and contact potential studies. Review of Scientific Instruments, 1995, 66, 4566-4574.	1.3	51